International Journal of Nanomedicine

Dovepress
open access to scientific and medical research

Open Access Full Text Article

ORIGINAL RESEARCH

Tunable and noncytotoxic PET/SPECT-MRI multimodality imaging probes using colloidally stable ligand-free superparamagnetic iron oxide nanoparticles

This article was published in the following Dove Press journal:
International Journal of Nanomedicine
27 January 2017
Number of times this article has been viewed

TH Nguyen Pham[1]
Nigel A Lengkeek[2]
Ivan Greguric[2]
Byung J Kim[1]
Paul A Pellegrini[2]
Stephanie A Bickley[3]
Marcel R Tanudji[3]
Stephen K Jones[3]
Brian S Hawkett[1]
Binh TT Pham[1]

[1]Key Centre for Polymers and Colloids, School of Chemistry, University of Sydney, [2]Radioisotopes and Radiotracers, NSTLI, Australian Nuclear Science and Technology Organisation, Sydney, [3]Sirtex Medical Limited, North Sydney, NSW, Australia

Abstract: Physiologically stable multimodality imaging probes for positron emission tomography/single-photon emission computed tomography (PET/SPECT)-magnetic resonance imaging (MRI) were synthesized using the superparamagnetic maghemite iron oxide (γ-Fe_2O_3) nanoparticles (SPIONs). The SPIONs were sterically stabilized with a finely tuned mixture of diblock copolymers with either methoxypolyethylene glycol (MPEG) or primary amine NH_2 end groups. The radioisotope for PET or SPECT imaging was incorporated with the SPIONs at high temperature. $^{57}Co^{2+}$ ions with a long half-life of 270.9 days were used as a model for the radiotracer to study the kinetics of radiolabeling, characterization, and the stability of the radiolabeled SPIONs. Radioactive $^{67}Ga^{3+}$ and Cu^{2+}-labeled SPIONs were also produced successfully using the optimized conditions from the $^{57}Co^{2+}$-labeling process. No free radioisotopes were detected in the aqueous phase for the radiolabeled SPIONs 1 week after dispersion in phosphate-buffered saline (PBS). All labeled SPIONs were not only well dispersed and stable under physiological conditions but also noncytotoxic in vitro. The ability to design and produce physiologically stable radiolabeled magnetic nanoparticles with a finely controlled number of functionalizable end groups on the SPIONs enables the generation of a desirable and biologically compatible multimodality PET/SPECT-MRI agent on a single T2 contrast MRI probe.

Keywords: magnetic resonance imaging, positron emission tomography, single-photon emission computed tomography, SPIONs, radiolabeling

Introduction

Over the last two decades, nanotechnology has been extensively developed and applied in the field of imaging technology. Compared to the conventional use of single molecules as contrast agents for in vivo and in vitro imaging, nanoparticles and nanoparticulate assemblies offer significant advantages and are providing important contributions to the field of diagnostic and noninvasive molecular imaging. Due to their high surface area-to-volume ratio, a higher amount of the desired payload can be incorporated with the contrast-generating nanoparticles/nanoparticulates, resulting in great improvements in the detection capability. Nanoparticles may allow imaging technologies to achieve a higher level of both anatomical and biological information with the use of a single probe.

The most popular dual-modality imaging technique in research involves a combination of UV/visible absorbance and/or fluorescence with magnetic resonance imaging (MRI). Nanoparticles with inherent optical properties, such as gold and quantum dots, have been labeled with a fluorophore or with an MRI contrast agent,

Correspondence: Brian S Hawkett; Binh TT Pham
School of Chemistry, The University of Sydney, Building F11, Eastern Avenue, Sydney, NSW 2006, Australia
Tel +61 2 9351 6973; +61 2 9351 6704
Fax +61 2 9351 8651
Email brian.hawkett@sydney.edu.au; binh.pham@sydney.edu.au

submit your manuscript | www.dovepress.com
Dovepress
http://dx.doi.org/10.2147/IJN.S127171

allowing their position to be pinpointed via MRI, while providing information on their environment via optical fluorescent signals.[1–7] Despite the disadvantages of using a negative contrast agent (T2 weighted) in MRI, due to the low signal-to-noise ratio, significant advances over the last 25 years have made the use of magnetic nanoparticles as T2 contrast agents preferable to the use of nanoparticles as T1-weighted contrast agents. Iron oxide magnetic nanoparticles, due to their inherent magnetic properties and feasibility to produce iron oxide cores, are the most common negative (T2 weighted) contrast agents and have been widely applied to in vitro and in vivo studies.[8–12] Among the dual-modality approaches, positron emission tomography/single-photon emission computed tomography (PET/SPECT)-MRI technologies offer high spatial resolution (~50 μm),[13] the best soft tissue contrast, the highest sensitivity, and detection limit.[14] The most common radionuclide probes applied as radiotracers or therapeutic agents in preclinical and clinical practice are ^{18}F, ^{64}Cu, ^{67}Ga, ^{68}Ga, ^{89}Zr, ^{90}Y, ^{124}I, ^{99m}Tc, ^{111}In, and ^{177}Lu.[12,15–18] These radionuclides have been incorporated into nanoparticles via coordination bonds with suitable functional groups or chelating ligands on the nanoparticles.

Despite the fact that hybrid PET/SPECT-MRI technologies have been emerging as new tools utilizing molecular probes for in vivo biomolecular and cellular imaging, as well as (pre-) clinical imaging in medical theranostics (a combination of therapy and diagnostics), a number of challenges in the production and performance of suitable and safe multimodality probes remain. The first challenge is the manufacture of imaging probes for clinical application. Robust synthesis, uniformity, batch-to-batch reproducibility, scaling-up, and colloidal stability remain aspects to be developed and optimized.[19] The second and most concerning challenge is probe biosafety, in particular their side effects when used in vivo and in clinical applications. Recently, systemic fibrosis was detected in clinical patients who had previously undergone administration of imaging contrast agents for MRI scans.[9,20,21] This side effect is suggested to be associated with the loss of toxic metal ions from the contrast agents.[20] In March 2015, the US Food and Drug Administration issued a report warning about the application of Feraheme™ (AMAG Pharmaceuticals, Lexington, MA, USA), an iron oxide-based product, in the treatment of anemia due to a number of reported serious side effects in patients.[22] These challenges are likely the reason why nanoparticle platforms remain limited to preclinical use, despite their potential applications in theranostics.[23]

Our previous studies showed that the sterically stabilized superparamagnetic iron oxide nanoparticles (s-SPIONs) were stable under physiological conditions, noncytotoxic in vitro, and have shown potential biomedical applications in drug delivery and stem cell tracking.[11,24] Our recent publication further demonstrated that these sterically stabilized SPIONs were highly stable and well dispersed after being mixed with fresh human red blood cells.[25] This work presents a robust aqueous-based production of multimodality PET/SPECT-MRI probes on single core superparamagnetic iron oxide (maghemite γ-Fe_2O_3) nanoparticles (SPIONs). Two types of sterically stabilized SPIONs are used in this study: 10 nm diameter (small core) and 25 nm diameter (big core) SPIONs with T2 relaxivity values of 368 $s^{-1}mM^{-1}$ and 953 $s^{-1}mM^{-1}$, respectively.[10,11] This potentially offers better negative MRI contrast agents than all commercially and clinically available samples of similar core sizes. Ligand-free radiolabeling, which was developed recently for commercially available iron oxide nanoparticles with PET radiotracers,[26,27] is applied to incorporate metal ions of Co, Ga, and Cu as models for PET/SPECT radiotracers. Radiolabeling kinetics, stability, and cytotoxicity of the radiolabeled SPIONs are also investigated.

Materials and methods

Materials

Two different core sizes of the maghemite iron oxide (γ-Fe_2O_3) with average diameter of 10 nm (SPION10) and 25 nm (SPION25) were used in this study. The SPIONs were sterically stabilized with a mixture of 5% NH_2 and 95% methoxypolyethylene glycol (MPEG, molar ratio) end functionalized macro-reversible addition fragmentation chain transfer (RAFT) blocks as reported in our previous publication[11,24] and referred to herein as s-SPION10 and s-SPION25. All the SPION samples, both uncoated and coated particles, were diluted with Milli-Q water to a concentration of 1 wt% prior to radiolabeling.

Cobalt(II) nitrate hexahydrate ($Co(NO_3)_2{\cdot}6H_2O$, 99.999% trace metals basis), gallium(III) chloride ($GaCl_3$, 99.999% trace metals basis), copper(II) nitrate trihydrate ($Cu(NO_3)_2{\cdot}3H_2O$, >99%), and hydrochloric acid (HCl, 30%–35%, TraceSELECT® Ultra) were purchased from Sigma-Aldrich (St. Louis, MO, USA). Milli-Q water was used throughout this work. Cell culture media were purchased from Thermo Fisher Scientific (Waltham, MA, USA). All cell lines used in the in vitro tests were from ATCC (Manassas, VA, USA). Cobalt-57 chloride ($^{57}CoCl_2$) in 0.02 M hydrochloric acid was purchased from Perkin Elmer (Waltham, MA, USA). Gallium-67 chloride ($^{67}GaCl_3$) in 0.1 M hydrochloric acid suitable for radiochemistry was produced from gallium-67 citrate for injection (Lantheus Medical Imaging, Billerica, MA, USA) using established

procedures.[28] Copper-64 chloride ($^{64}CuCl_2$) in 0.02 M HCl was obtained from RAPID Labs, SCGH (Perth, Australia).

Experimental methods

Labeling the sterically stabilized SPIONs with Co^{2+}, Ga^{3+}, and Cu^{2+}

Scheme 1 shows the chemical structures and schematic pictures of the stabilized SPIONs. All of the SPION samples, both uncoated and coated particles, were diluted with Milli-Q water to a concentration of 1 wt% prior to labeling.

Reactions of SPIONs (1 wt%, 50 µL) with Co(II) nitrate, Ga(III) chloride, or Cu(II) nitrate (1 mM in 0.1 M HCl, 40 µL) were carried out at different pH values and temperatures. Sodium acetate buffers (pH 4, 4.5, 5, 5.5, and 1.0 M) and sodium acetate (1.0 M) were added to the reaction mixtures to the final concentrations of 0.1 M. The reaction mixtures (400 µL) were then heated at either 75°C or 95°C using an oil bath for 30 min, after which the free metal ions were separated from the SPIONs by centrifuging at 10,000 rpm for 30 min. After removing supernatant, the SPIONs were washed twice with Milli-Q water and then redispersed in 400 µL Milli-Q water. Metal concentrations in the reaction mixtures, supernatants, and products were analyzed by graphite furnace atomic absorption spectroscopy (GF-AAS).

Radiolabeling of SPIONs with ^{57}Co and ^{67}Ga

Preparation of $[^{57}Co/^{natural\ (nat)}Co]^{2+}$ radiotracer stock solution

Serial solutions of $Co(NO_3)_2$ (0.10, 1.0, and 10 mM in 0.1 M HCl) were prepared by diluting 0.1 M $Co(NO_3)_2$ stock (2.91 g $Co(NO_3)_2{\cdot}6H_2O$ in 10 mL of 0.1 M HCl) in 0.1 M HCl. An aliquot of ^{57}Co in 0.1 M HCl (~7 MBq) was mixed with the stock solutions of $Co(NO_3)_2$ (0.1 or 1 mM) to give a final activity of ~300 kBq per reaction prior to the radiolabeling.

Radiolabeling of SPIONs

Each radiolabeling experimental condition was carried out in triplicate to establish the reproducibility of the applied process.

Radiolabeling of SPIONs with $[^{57}Co/^{nat}Co]^{2+}$ (~1 kBq/nmol) was carried out in sodium acetate buffer (final concentration of 0.1 M). Typically, an aliquot of 1.0 M sodium acetate (40 µL) was added into an acid-washed 1.5 mL microcentrifuge tube, followed by the addition of Milli-Q water (300 µL), $[^{57}Co/^{nat}Co]^{2+}$ tracer solution, and 1 wt% SPION suspension (50 µL, 0.5 mg of Fe). The reaction mixture was placed on a heating block at a targeted temperature for 30 min. After cooling for 10 min, 20 µL of reaction mixture was aliquoted from the reaction mixture, and the radioactivity was measured using a gamma counter. The remaining portion was centrifuged at 10,000× *g* for 20 min. Then, 20 µL of the supernatant, containing unreacted $[^{57}Co/^{nat}Co]^{2+}$, was aspirated out to measure the radioactivity; the remaining supernatant was discarded. The radiolabeled SPIONs were redispersed in Milli-Q water using a sonic bath for 10 min. The control samples were prepared, in which the volume of SPIONs was replaced by Milli-Q water. The radiolabeling efficiencies were calculated as the percentages of (total radioactivity − radioactivity of supernatant)/total radioactivity.

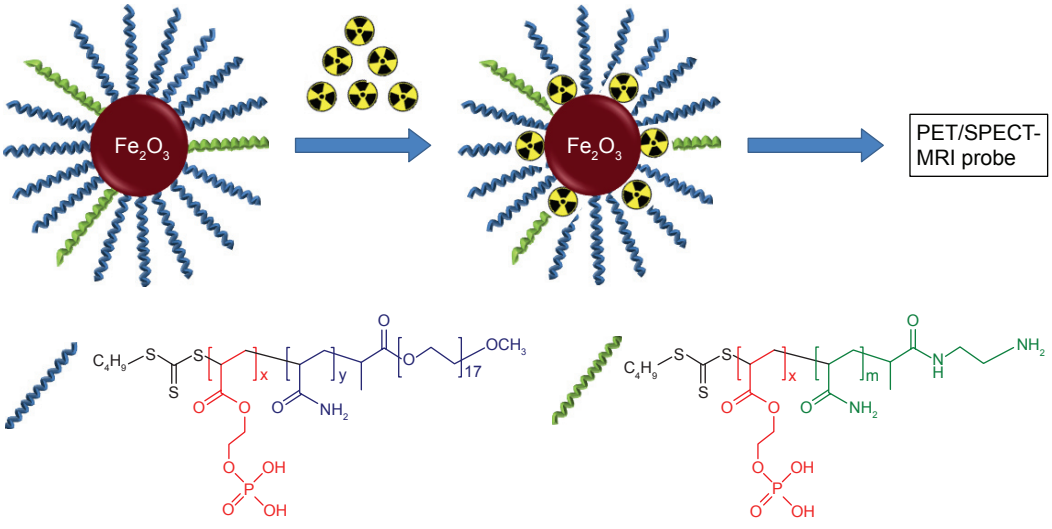

Scheme 1 Schematic composition of the sterically stabilized SPIONs and the radiolabeled products.
Notes: The steric stabilizers for SPIONs contained anchoring phosphate blocks (red) to iron oxide core surface and stabilizing blocks of 95% (by molar ratio) MPEG (blue) and 5% NH_2 end functionalized polyacrylamide (green) (x=6; y=0 and 40 for small and big cores, respectively; m=20 and 60 for small and big cores, respectively).
Abbreviations: SPIONs, superparamagnetic iron oxide nanoparticles; MPEG, methoxypolyethylene glycol; PET, positron emission tomography; SPECT, single-photon emission computed tomography; MRI, magnetic resonance imaging.

A similar procedure was also applied for the labeling of SPIONs with $^{67}Ga^{3+}$ and (nonradioactive) Cu^{2+} unless stated otherwise.

Stability studies in physiological media

Radiolabeled SPIONs were redispersed in different media, including 0.9% saline, phosphate-buffered saline (PBS), or 5% glucose solution, by sonication for 10 min to check their dispersity. The dispersions were maintained at room temperature for up to 7 days to check their stability. At various time intervals, the dispersions were centrifuged at 10,000 rpm for 20 min. Then, 20 µL of the dispersion (before centrifugation) and of the supernatant (after centrifugation) were collected to measure radioactivity on the gamma counter. The particles pellet was redispersed in the media via sonication.

Characterization methods

Dynamic light scattering (DLS) and transmission electron microscopy (TEM)

A DLS instrument (Zetasizer nanoseries, helium–neon laser at 633 nm, 40 mW; Malvern Instruments, Malvern, UK) with a detection angle of 173° was used to measure the particle sizes. Samples were measured at 25°C. The particles were dispersed in Milli-Q water or PBS at 0.5 mg/mL prior to measurement.

TEM analysis was performed in a JEOL 1400 at an accelerating voltage of 200 kV. A diluted sample (about 10 µg/mL in water) of SPIONs was drop casted onto a 200 meshed carbon-coated Formvar™ copper TEM grid and air-dried before imaging.

Atomic absorption spectroscopy (AAS) to measure metal contents in SPIONs

The iron content in the SPIONs was measured using an AAS instrument (Varian AA800 spectrometer, with acetylene/air flame atomization). An iron standard solution (1,000 mg/L in HNO_3; Merck, Darmstadt, Germany) was used for the calibration curve. Samples of dried SPIONs were digested in nitric acid (trace analysis grade, EM-1.00441.1000, 65% [w/v]; Millipore, Billerica, MA, USA), followed by a dilution with 0.1 M HCl (Merck) prior to the measurement.

Concentrations of cobalt, gallium, and copper were analyzed using a GF-AAS (Agilent 240FS AA spectrometer with a Zeeman graphite tube atomizer). The standard solutions of Co(II), Ga(III), and Cu(II) at 25, 50, and 40 ppb, respectively, in 0.1 M HCl were used for the calibration curve of each element.

Gamma Counter to measure radioactivity of the radiolabeled SPIONs

The radiolabeling efficiency for SPIONs labeled with ^{57}Co or ^{67}Ga, under different conditions, was determined by gamma counting of the particles and supernatant solutions using a Gamma Counter (Wizard 2480; Perkin Elmer). The particles suspension in an Eppendorf tube was centrifuged at 14,000× *g* for 20 min to obtain clear supernatant. Then, 10 µL of the particle suspension or the supernatant from each SPION sample, in triplicate, was placed in a glass culture tube (6×50 mm), and the radioactivity was measured on a gamma counter (300 s count time for each measurement).

Cell culture and viability assay

3T3-L1 and L6 cells (kind gifts from Dr Aviva Levina) were maintained as confluent monolayers in Dulbecco's Modified Eagle's Medium (DMEM, 10566-016; Gibco, Grand Island, NY, USA), supplemented with 10% (v/v) fetal calf serum (FCS). The cells were incubated under standard culturing conditions (at 37°C with 5% [v/v] CO_2 under humidified conditions). Cells were routinely subcultured by removal of the medium, washing with PBS (IVT3001302; In Vitro Technologies, Noble Park North, VIC, Australia), and detached from the culture-ware by 0.25% (w/v) trypsin (59430C; SAFC Biosciences, Brooklyn, VIC, Australia). The cell suspension was collected in a centrifuge tube with the addition of complete growth medium and spun down at ~1,000 rpm for 3 min. The supernatant was discarded, and the cells were resuspended in fresh growth medium. Cells were then counted on a hemocytometer, and an appropriate number of cells were seeded for further experiments and subculturing.

A total of 1×10^5 cells/well suspension was seeded into each well of a 96-well plate (3599; Corning, Kennebunk, ME, USA) and incubated for 24 h under standard culturing conditions. Prior to the assay, SPION suspensions, including *Cu*-s-SPION10, *Cu*-s-SPION25, *Ga*-s-SPION10, and *Ga*-s-SPION25, were sterilized by filtration with a hydrophilic regenerated cellulose 0.22 µm filter. The dose volume of the nanoparticles was kept <24% of the total volume. A sample of the filtered particles in cell media at a desired concentration was processed for AAS to confirm the concentration of SPIONs applied to cells. The filtered particles were diluted in complete culture medium and added to triplicate wells spanning a 3-log range of final concentrations (250, 125, 62.5, 31.2, 15.6, 7.81, and 3.91 ppm, unless otherwise stated). The cells were then incubated for 24 or 72 h before 1.0 mM thiazolyl blue tetrazolium bromide (MTT; L11939; Alfa Aesar, Heysham, UK) was added and further incubated for 4 h. The media was removed, and 200 µL of dimethyl sulfoxide (DMSO; Sigma-Aldrich) was added to each well. The absorbance at 600 nm was then measured for the plate in a Victor^{3}V microplate reader (1420; Perkin Elmer). IC_{50}

values were determined as the drug concentration that reduced the absorbance to 50% of that in untreated control wells.

Results and discussion

Quantitative measurements of Co^{2+} concentration on SPIONs

Radiolabeling of SPIONs with $[^{57}Co/^{nat}Co]^{2+}$: effect of pH and temperature

Initially we investigated suitable and optimum conditions for radiolabeling. The first parameter we investigated was pH. Inorganic bases are often used to adjust the pH for radiolabeling reactions by many research groups.[26,27] Then, 0.1 M NaOH was first used to adjust the pH of the reaction mixture to 8.0. However, the use of NaOH resulted in the pH becoming excessively high and causing precipitation of $Co(OH)_2$ in the reaction mixture. As shown in Figure 1A, in the control sample without the presence of SPIONs, an extremely low level of activity (10% of the total) was detected in the supernatant after centrifugation when using NaOH to adjust the pH, whereas when using 0.1 M sodium acetate directly to obtain pH 8, ~100% of the total activity remained in the supernatant after centrifugation.

The radiometal labeling was also influenced by the pH of the reaction mixture. When using sodium acetate buffer, increasing pH (from 4.0 to ~8.0), at the same reaction temperature of 95°C, resulted in a marked improvement in radiochemical yield for the radiolabeling of SPIONs with $[^{57}Co/^{nat}Co]^{2+}$. Experimental data shown in Figure 1B illustrate that under low pH conditions (acetate buffer, pH =4.0–5.5), low radiochemical yields, <20%, were obtained for s-SPION10. The highest radiolabeling efficiency (~77%) was obtained when the reaction was carried out using 0.1 M sodium acetate at pH ~8. A range of temperatures were also studied to find out an optimum reaction temperature for the labeling reaction. Results shown in Figure 1C illustrate that under the pH 8.0 acetate buffer as the optimum buffer, increasing temperature also significantly improved radiochemical yield for both s-SPION10 and s-SPION25. At room temperature (25°C), the radiochemical yield with $[^{57}Co/^{nat}Co]^{2+}$ only reached 26% and 10% for s-SPION10 and s-SPION25, respectively. When heating the reaction mixtures to 75°C for 30 min, the radiochemical yield was ~75% and 40% yield for s-SPION10 and s-SPION25, respectively. The highest radiochemical yields, ~75% and 57% for s-SPION10 and s-SPION25, respectively, were

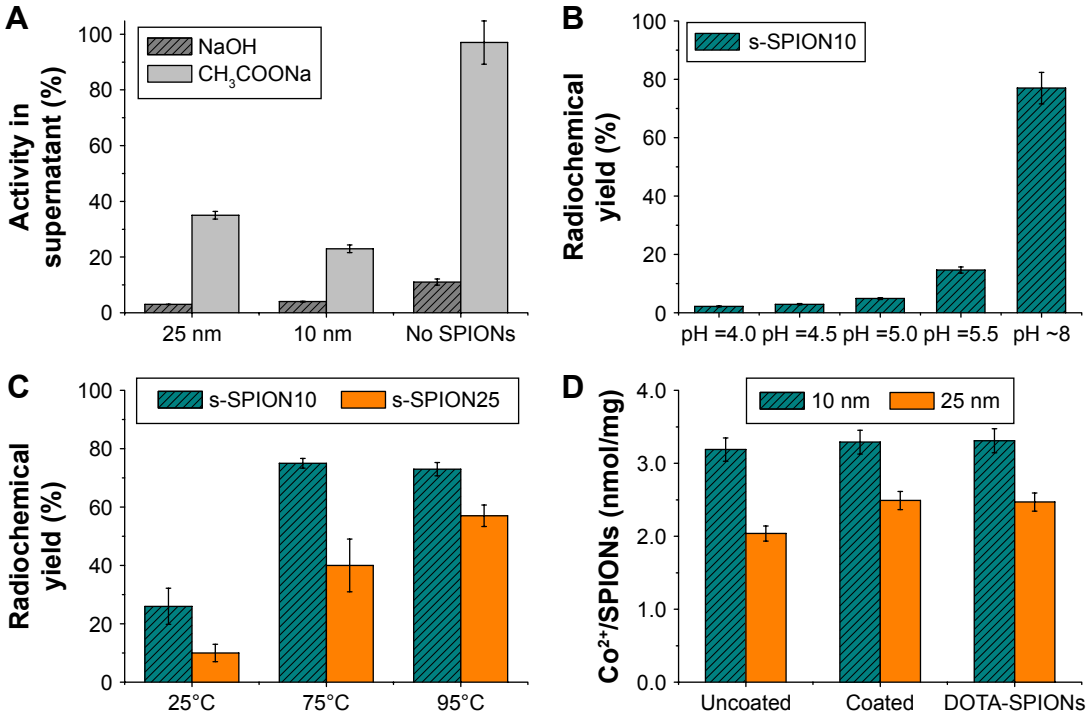

Figure 1 Radiolabeling SPIONs with radioactive cobalt.

Notes: Dispersion of SPIONs (1 wt%, 50 µL, s-SPION10 or s-SPION25) was added into a solution of $[^{57}Co/^{nat}Co]^{2+}$ (~10 KBq, $[^{nat}Co^{2+}]$ =2 nmol) in (**A**) 0.1 M sodium acetate (pH ~8) or water with pH adjusted to 8 using 0.1 M NaOH, heated at 95°C for 30 min; (**B**) 0.1 M acetate buffer at different pH (4–8), heated at 95°C for 30 min; (**C**) 0.1 M sodium acetate (pH ~8), heated at different temperatures of 25, 75, or 95°C for 30 min; and (**D**) 0.1 M sodium acetate (pH ~8), heated to 95°C for 30 min. Error bars = standard errors, n=3.

Abbreviations: nat, natural; DOTA-SPIONs, s-SPIONs with DOTA (1,4,7,10-tetraazacyclododecane-1,4,7,10-tetraacetic acid) as chelating ligand conjugated to the NH_2 end group of the stabilizer; SPIONs, superparamagnetic iron oxide nanoparticles; s-SPIONs, stabilized SPIONS; s-SPION10, s-SPIONs with average core diameter of 10 nm; s-SPION25, s-SPIONs with average core diameter of 25 nm.

obtained when the reaction mixtures were heated at 95°C for 30 min. As the same amount of iron oxide mass was used in all cases, the number of particles, ie, the number of reaction sites, for the smaller size particles was significantly higher than that for the bigger ones. This resulted in the higher radiochemical yield for s-SPION10 under the same conditions. From these results, a temperature of 95°C and 0.1 M sodium acetate, pH 8.0, were chosen for the radiolabeling of SPIONs with $[^{57}Co/^{nat}Co]^{2+}$ for further studies.

As the SPIONs were coated with polymer blocks that could potentially chelate to metal ions, it is important to determine whether the $[^{57}Co/^{nat}Co]^{2+}$ ions bind to the nanoparticle surface or the polymer-coating layers. The uncoated SPIONs, the coated SPIONs as well as the coated SPIONs with 1,4,7,10-tetraazacyclododecane-1,4,7,10-tetraacetic acid as chelating ligand conjugated to the NH_2 end group of the stabilizer (DOTA-SPIONs) were labeled with $[^{57}Co/^{nat}Co]^{2+}$ using the same conditions; 0.1 M sodium acetate, at 95°C for 30 min. The radioactivity obtained on the nanoparticles (Figure 1D) was similar between three particle types, ~3.3 and 2.5 nmol of Co^{2+}/mg of 10 and 25 nm SPIONs, respectively. This result strongly indicates that Co^{2+} ions are likely deposited on the surface of the iron oxide core, even in the presence of additional chelating ligands.

Loading capacity of $[^{57}Co/^{nat}Co]^{2+}$ on s-SPIONs

To further investigate the metal binding capacity of Co^{2+} on the s-SPIONs, fixed amounts of s-SPIONs (0.5 mg) were added into reaction mixtures with increasing ratios of $^{nat}Co^{2+}/^{57}Co^{2+}$ (Figure 2). To minimize the use of higher radioactivity level, we did not aim to extend the duration of a radiolabeling reaction. Thus, we chose a reaction time of 30 min and evaluated the optimum concentration and conditions to achieve a highest possible radiolabeling yield. The fixed amount of $^{57}Co^{2+}$ would act as a radiotracer for the experiment. Once the loading limit of $^{nat}Co^{2+}$ loading was reached, increasing levels of $^{57}Co^{2+}$ would be found in the supernatant. The reaction conditions were maintained constant; 95°C for 30 min; the amount of $[^{57}Co/^{nat}Co]^{2+}$ led to an elevated level of $[^{57}Co/^{nat}Co]^{2+}$ in the product (Figure 2A). As expected, the radiochemical yield decreased with increasing ratios of $^{nat}Co^{2+}$ to $^{57}Co^{2+}$ (Figure 2B). Using 400 nmol of $^{nat}Co^{2+}$/mg of s-SPIONs gave ~170 nmol (yield 42%) and 110 nmol (yield 28%) $[^{57}Co/^{nat}Co]^{2+}$/mg of s-SPION10 and s-SPION25, respectively. Meanwhile, the radiochemical yields reached 90% for s-SPION10 and 71% for s-SPION25 within 30 min of reaction time when only 2 nmol of $[^{57}Co/^{nat}Co]^{2+}$/mg of s-SPIONs were used.

Stability of $[^{57}Co/^{nat}Co]^{2}$ labeled-SPIONs ($[^{57}Co/^{nat}Co]^{2+}$-s-SPIONs) in simulated physiological conditions

As anticipated, the experimental data showed that the radiolabeled nonstabilized SPIONs were not dispersible at all in aqueous phases. The particles coagulated and/or aggregated and settled down to the bottom of the vial rapidly. Any aggregation or flocculation of particles under physiological conditions would cause the blocking of blood vessels or local retention of particles upon treatment and therefore result in an acute toxicity of the particles.

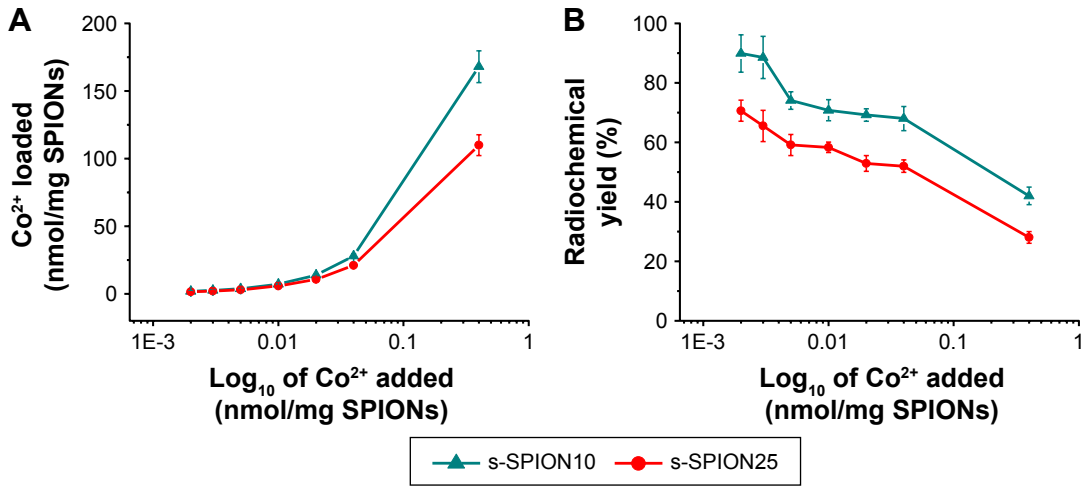

Figure 2 Loading capacity of Co^{2+} on s-SPIONs after the reaction for 30 min at 95°C in 0.1 M sodium acetate.
Notes: (**A**) amounts of Co^{2+} loaded on s-SPIONs (nmol/mg of dry s-SPIONs) and (**B**) labeling yield (%) when increasing the amounts of $^{57}Co/Co^{2+}$ added in the reaction mixtures. Error bars = standard errors, n=3.
Abbreviations: SPIONs, superparamagnetic iron oxide nanoparticles; s-SPIONs, stabilized SPIONs; s-SPION10, s-SPIONs with average core diameter of 10 nm; s-SPION25, s-SPIONs with average core diameter of 25 nm.

On the other hand, due to the coating layer of steric stabilizers, radiolabeling the s-SPIONs did not alter the aqueous-phase dispersability of the initial s-SPIONs. During the radiolabeling, the s-SPIONs remained well dispersed under the harsh reaction conditions, including high concentration of buffer and high temperature (Figure 3A). Radiolabeled s-SPIONs could be easily resuspended and were stable in various aqueous dispersing media, including water, 0.9% saline, and PBS. The AAS results for the filtered s-SPIONs and labeled s-SPIONs (data not shown) showed that the concentration of iron given by SPIONs did not change after being filtered through a sterile 0.22 μm filter (to sterile SPIONs for in vitro cytotoxicity tests), which is another solid evidence of the well dispersed and stable s-SPIONs.

Retention of the radionuclide with the vector is a critical aspect of radiotracer development. Loss of the radionuclide may result in localization in untargeted tissue or untimely excretion, thus it is important that the radionuclides remain bound to the particles. We investigated this property of our particles by incubation of $[^{57}Co/^{nat}Co]^{2+}$-s-SPIONs in water, saline, and PBS for 24 h. We observed that <2% of the total activity was leached out from the cores during this time period, indicating very stable binding of the radiometal (Figure 3B).

Labeling s-SPIONs with PET/SPECT agents

With the optimization of radiolabeling conditions and the excellent stability of ^{57}Co-s-SPIONs, we investigated the radioisotopes potentially useful as SPECT and PET imaging agents, ^{67}Ga and ^{64}Cu, respectively.

s-SPIONs labeled with ^{67}Ga

Similar conditions were applied to investigate the reaction between s-SPIONs and ^{67}Ga. In this study, a mixture of $[^{67}Ga/^{nat}Ga]^{3+}$ was prepared by adding 10 μL of ^{67}Ga (~2.5 MBq, chloride form in 0.1 M HCl) to 200 μL of 0.1 mM Ga(III) nitrate solution in 0.1 M HCl. The reaction was carried out at either pH 5.5 (0.1 M acetate buffer) or pH 8 (0.1 M sodium acetate) and heated at 95°C for 30 min. The radiochemical yield was found to be almost quantitative (100%) at both pHs and for both s-SPION10 and s-SPION25 (Figure 4A).

Studying the reactions of s-SPIONs with nonradioactive Cu^{2+} and Ga^{3+} and the stability of the products

The high labeling efficiency of s-SPIONs with ^{57}Co and ^{67}Ga and the stability of the products have been demonstrated. These studies were repeated using nonradioactive cations, including Cu^{2+} and Ga^{3+}. Furthermore, the colloidal properties of the s-SPIONs, including particle size and stability, and the toxicity of the labeled s-SPIONs were also studied. The amount of metal cations was quantified by GF-AAS. The reactions with Cu^{2+} or Ga^{3+} at different pHs and temperatures were only performed with s-SPION25 (Figure 4B and C). The control reactions, in which no s-SPION25 was added, were carried out simultaneously to monitor for the precipitation of metal oxide or hydroxide in the higher pH buffers. Under all studied conditions, 100% of added metal cations were found to remain in the supernatant after centrifugation (data not shown). Similar to what we observed in radioactive labeling

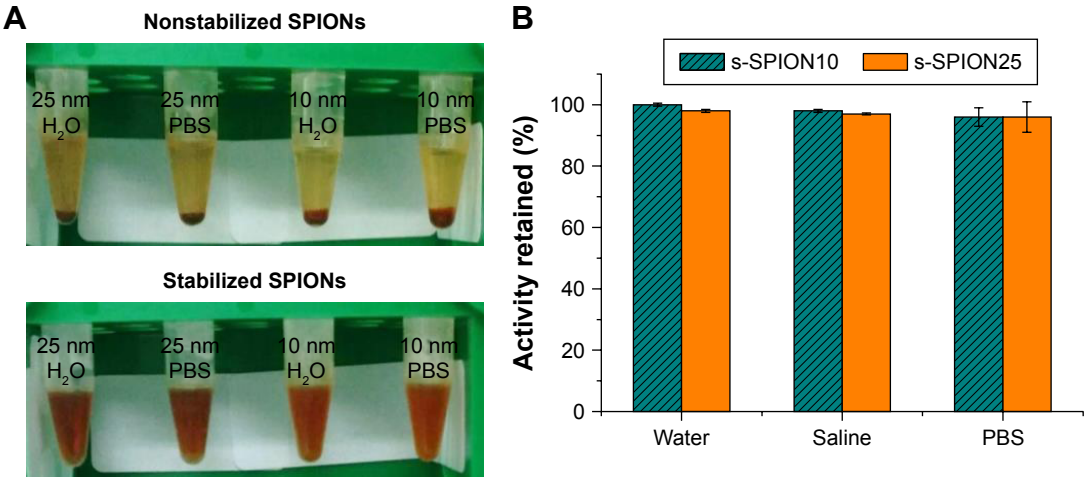

Figure 3 Colloidal and radiochemical stability of SPIONs.
Notes: (**A**) Well dispersion of the stabilized SPIONs in water and PBS after labeling with ^{57}Co (bottom) in contrast to the unstabilized SPIONs (top) and (**B**) the activity of ^{57}Co remained on $[^{57}Co/^{nat}Co]^{2+}$-s-SPIONs after 24 h under physiological conditions. Error bars = standard errors, n=3.
Abbreviations: nat, natural; SPIONs, superparamagnetic iron oxide nanoparticles; s-SPIONs, stabilized SPIONs; s-SPION10, s-SPIONs with average core diameter of 10 nm; s-SPION25, s-SPIONs with average core diameter of 25 nm; NP, nanoparticle; PBS, phosphate-buffered saline.

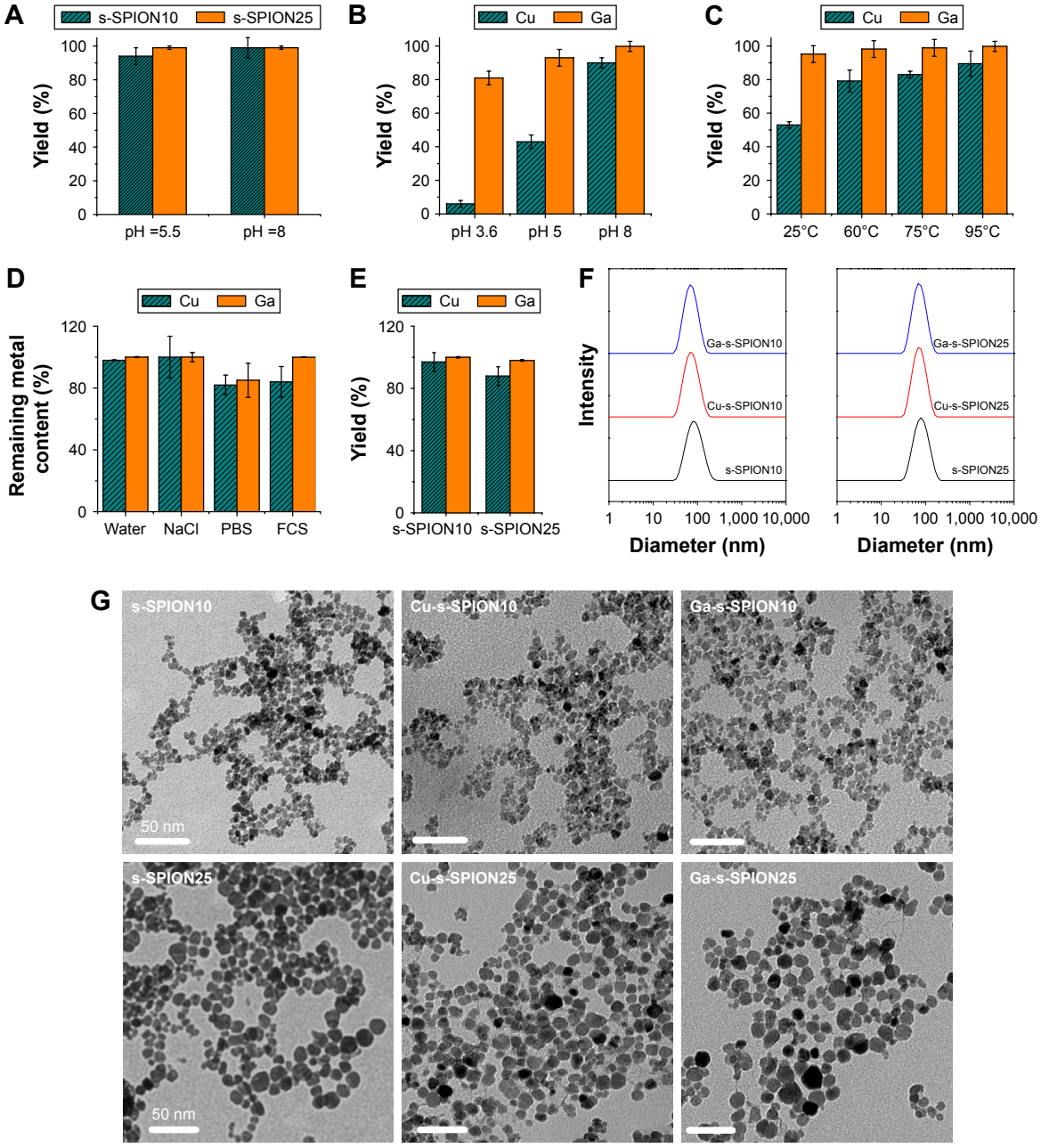

Figure 4 Labeling s-SPIONs with Ga and/or Cu.

Notes: (**A**) Labeling efficiency of s-SPIONs (1 wt%, 50 μL, s-SPION10 or s-SPION25) with [$^{67}Ga/^{nat}Ga$]$^{3+}$ (~125 KBq, 1 nmol Ga^{3+}) at pH 5.5 (0.1 M acetate buffer) or at pH 8 (0.1 M sodium acetate), heating at 95°C for 30 min. (**B** and **C**) Labeling efficiency of s-SPION25 with Cu^{2+} and Ga^{3+} (in 0.1 M sodium acetate at different pHs, heating at 95°C for 30 min, and at different temperatures, pH 8, for 30 min). Constant amounts of 0.5 mg s-SPIONs and 1 nmol of metal ions were used in all reactions. (**D**) Stability of *Cu*-s-SPION25 and *Ga*-s-SPION25 after 24 h incubation in different media represented by the percentages of Cu or Ga remained bound to nanoparticles. (**E**) Co-labeling of s-SPIONs with Cu^{2+} and Ga^{2+} at 95°C after 30 min resulted in ~100% yield for both metal cations. (**F**) DLS of s-SPIONs before and after labeling with Ga^{3+} or Cu^{2+} did not show any changes in the hydrodynamic size. (**G**) Transmission electron micrographs of the sterically stabilized particles before labeling (s-SPION10 and s-SPION25) and after labeling with Cu^{2+} (*Cu*-s-SPION10 *and Cu*-s-SPION25) or with Ga^{3+} (*Ga*-s-SPION10 and *Ga*-s-SPION25); scale bars: 50 nm. Error bars = standard errors, n=3.

Abbreviations: Cu-s-SPION10, s-SPIONs with average core diameter of 10 nm and labeled with Cu; Ga-s-SPION10, s-SPIONs with average core diameter of 10 nm and labeled with Ga; Cu-s-SPION25, s-SPIONs with average core diameter of 25 nm and labeled with Cu; Ga-s-SPION25, s-SPIONs with average core diameter of 25 nm and labeled with Ga; SPIONs, superparamagnetic iron oxide nanoparticles; s-SPIONs, stabilized SPIONs; s-SPION10, s-SPIONs with average core diameter of 10 nm; s-SPION25, s-SPIONs with average core diameter of 25 nm; PBS, phosphate-buffered saline; FCS, fetal calf serum; DLS, dynamic light scattering.

with ^{67}Ga, the reaction of Ga^{3+} with s-SPION25 was less pH and temperature dependent. The reaction yields after heating to 95°C at pH 5 and 8 were ~93% and ~99%, respectively (Figure 4B). The yield obtained at pH 3.6 was slightly lower (~80%). Using 0.1 M sodium acetate (pH ~8), ~100% of Ga^{3+} added in the reaction mixture bound to s-SPION25 not only at 95°C but also at 25°C, 60°C, and 75°C (Figure 4C). In contrast, the reaction of s-SPION25 with Cu^{2+} was strongly pH and temperature dependent as shown in Figure 4B and C. The labeling process required high temperature and high pH

in order to obtain a high yield of the product. Specifically, in 0.1 M sodium acetate and heating at 95°C for 30 min, ~90% of added Cu^{2+} was deposited on the surface of s-SPION25.

The *Cu*-s-SPION25 and *Ga*-s-SPION25 were incubated for 24 h in various media including water, 0.9% saline, PBS, and 10% FCS to study the dissociation of Cu and Ga from SPIONs into the media. All samples remained dispersed in these media. GF-AAS analyses of Cu and Ga concentrations in the supernatant after centrifugation showed that <1% of both Cu and Ga were released from SPIONs in either water or saline (Figure 4D). Incubation of labeled s-SPIONs in PBS or FCS resulted in <10% of Ga and Cu leaching. However, this could be due to the presence of s-SPIONs still remaining in the supernatant after centrifugation as the errors were significant.

In addition, using this method, labeling s-SPIONs with both Cu^{2+} and Ga^{3+} for hybrid PET-SPECT imaging was successfully carried out. The multiradioisotope-labeled s-SPIONs offer high potential as all-in-one PET/SPECT-MRI agents. Applying reaction conditions that gave the highest efficacy for both Cu^{2+} and Ga^{3+}, 0.1 M sodium acetate and heating at 95°C for 30 min, using equal amounts of Cu^{2+} and Ga^{3+} (1 nmol) for the reaction with either s-SPION10 or s-SPION25 (0.5 mg), ~100% yield and >90% yield were achieved for Ga^{3+} and Cu^{2+}, respectively (Figure 4E).

The hydrodynamic size of the labeled s-SPIONs did not change after going through a tough preparation process involving high salt concentration, high temperature, and high-speed centrifugation (Figure 4F). The TEM images of the SPIONs before and after metal labeling (Figure 4G) showed that the labeling processes did not change the core size or the appearance of the particles significantly. The observed excellent stability properties of these s-SPIONs are crucial for nanomedicine applications as they should ensure their stability during preparation and future investigations in vivo.

It is worth noting that all (radio-)metal-labeling processes described above were robust and reproducible with very small standard errors (Figures 1–4).

Toxicity of the metal-labeled s-SPIONs in vitro

The toxicity of the s-SPION10 and s-SPION25 in various cell lines was described in our previous reports.[10,11,24] In order to study the safety of the labeled s-SPIONs by MTT assay, four samples of *Cu*-s-SPION10, *Cu*-s-SPION25, *Ga*-s-SPION10, and *Ga*-s-SPION25 were prepared in larger scale using 10 mg of s-SPION10 or s-SPION25 and 0.6 µmol of Cu^{2+} or Ga^{3+}. The reactions were carried out in 0.1 M acetate buffer (pH 8.0) at 95°C for 30 min, and then the labeled products were collected by centrifugation and washed three times with water prior to redispersing in 1 mL of water. The concentrations of Fe and Cu or Ga in the final products were quantified by GF-AAS. For the MTT assay, all four samples were diluted with saline to the final concentrations of 50 mM Fe, and concentrations of Cu and Ga are given in Table 1. The highest concentration of the labeled s-SPIONs tested on two cell lines was 3.0 mM of Fe (corresponding to 250 µg/mL Fe_2O_3). No cytotoxicity was observed on L6 muscle cells and 3T3-L1 preadipocytes at the highest concentration tested as shown in Figure 5.

Table 1 Concentrations of labeled s-SPIONs used in MTT assay for cell viability

Sample	[Fe] (mM)	[Cu] or [Ga] (µM)
Cu-s-SPION10	50	273
Ga-s-SPION10	50	282
Cu-s-SPION25	50	234
Ga-s-SPION25	50	241

Abbreviations: [Cu], copper concentration; [Fe], iron concentration; [Ga], Ga concentration; MTT, thiazolyl blue tetrazolium bromide; Cu-s-SPION10, s-SPIONs with average core diameter of 10 nm and labeled with Cu; Ga-s-SPION10, s-SPIONs with average core diameter of 10 nm and labeled with Ga; Cu-s-SPION25, s-SPIONs with average core diameter of 25 nm and labeled with Cu; Ga-s-SPION25, s-SPIONs with average core diameter of 25 nm and labeled with Ga; s-SPIONs, stabilized superparamagnetic iron oxide nanoparticles.

The good dispersity, stability in aqueous media, and noncytotoxicity of the sterically stabilized SPIONs, both before[10] and after labeling with radiometal and metal ions (as shown in this study), are essential requirements for imaging contrast agents in particular and for any further biomedical application in general.

Conclusion

SPIONs with excellent MRI-negative contrast were successfully radiolabeled with the SPECT radioisotope, ^{67}Ga, or with the PET radioisotope, ^{64}Cu, in acetate buffer. The radiochemical yields of radiolabeling with ^{57}Co were found to be strongly dependent on temperature and time for both raw ferro-fluid (unstabilized iron oxide cores) and sterically stabilized SPIONs. No detectable loss of radionuclides from the particles to the aqueous phase in various physiological media was observed. The sterically stabilized radiolabeled s-SPIONs were fully redispersed and remained stable in aqueous buffer solutions such as PBS (Figure 5) and were also shown to be noncytotoxic in vitro. These are crucial properties of nanoparticles for an injectable formulation in biomedical applications.

In addition to the synthesis of the well-defined PET/SPECT-MRI, our capability to synthesize SPIONs with heterogeneous coating, which consists of different end functional groups such as $–NH_2$ on the stabilizing molecules,[11,24] also

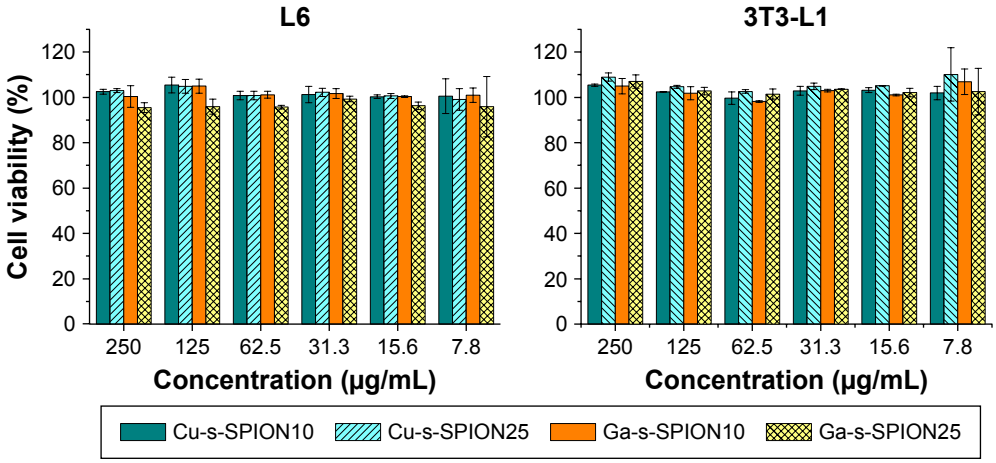

Figure 5 In vitro cytotoxicity tests for the metal-labeled SPIONs.
Notes: L6 (left) or 3T3-L1 (right) cell lines were treated with Cu/Ga-labeled s-SPIONs at the concentration of up to 250 μg/mL for 72 h. No significant toxicity was observed for all samples. Error bars = standard errors, n=3.
Abbreviations: SPIONs, superparamagnetic iron oxide nanoparticles; s-SPIONs, stabilized SPIONs; s-SPION10, s-SPIONs with average core diameter of 10 nm; s-SPION25, s-SPIONs with average core diameter of 25 nm.

enable us to carry out further postmodification with finely controlled amounts of an appropriate targeting agent and/or fluorescent imaging agent.

This study offers a robust and simple production for a potential next generation of nontoxic multimodality PET/SPECT-MRI single probe imaging agents.

Acknowledgments

The authors acknowledge the financial support from Sirtex Medical Ltd. and from AINSE grant (award number ALNGRA15522); and Dr Algi Serelis of DuluxGroup for RAFT reagents. The authors acknowledge the facilities and the technical assistance of the Australian Science and Technology Organisation (ANSTO), and of the Australian Microscopy & Microanalysis Research Facility (AMMRF) at the Australian Centre for Microscopy and Microanalysis (ACMM), The University of Sydney.

Disclosure

The authors report no conflicts of interest in this work.

References

1. Koo H, Huh MS, Sun IC, et al. In vivo targeted delivery of nanoparticles for theranosis. *Acc Chem Res*. 2011;44(10):1018–1028.
2. Kircher MF, Mahmood U, King RS, Weissleder R, Josephson L. A multimodal nanoparticle for preoperative magnetic resonance imaging and intraoperative optical brain tumor delineation. *Cancer Res*. 2003; 63(23):8122–8125.
3. Cormode DP, Skajaa T, van Schooneveld MM, et al. Nanocrystal core high-density lipoproteins: a multimodality contrast agent platform. *Nano Lett*. 2008;8(11):3715–3723.
4. Lin J-J, Chen J-S, Huang S-J, et al. Folic acid–pluronic F127 magnetic nanoparticle clusters for combined targeting, diagnosis, and therapy applications. *Biomaterials*. 2009;30(28):5114–5124.
5. Ke J-H, Lin J-J, Carey JR, Chen J-S, Chen C-Y, Wang L-F. A specific tumor-targeting magnetofluorescent nanoprobe for dual-modality molecular imaging. *Biomaterials*. 2010;31(7):1707–1715.
6. Pittet MJ, Swirski FK, Reynolds F, Josephson L, Weissleder R. Labeling of immune cells for in vivo imaging using magnetofluorescent nanoparticles. *Nat Protoc*. 2006;1(1):73–79.
7. Devaraj NK, Keliher EJ, Thurber GM, Nahrendorf M, Weissleder R. 18F labeled nanoparticles for in vivo PET-CT imaging. *Bioconjug Chem*. 2009;20(2):397–401.
8. Song H-T, Jordan EK, Lewis BK, et al. Rat model of metastatic breast cancer monitored by MRI at 3 Tesla and bioluminescence imaging with histological correlation. *J Transl Med*. 2009;7:88.
9. Lohrke J, Frenzel T, Endrikat J, et al. 25 years of contrast-enhanced MRI: developments, current challenges and future perspectives. *Adv Ther*. 2016;33(1):1–28.
10. Pham BTT, Jain N, Kuchel PW, et al. The interaction of sterically stabilized magnetic nanoparticles with fresh human red blood cells. *Int J Nanomedicine*. 2015;10:6645–6655.
11. Eamegdool SS, Weible MW 2nd, Pham BTT, Hawkett BS, Grieve SM, Chan-ling T. Ultrasmall superparamagnetic iron oxide nanoparticle prelabelling of human neural precursor cells. *Biomaterials*. 2014; 35(21):5549–5564.
12. Torres Martin de Rosales R, Tavaré R, Glaria A, Varma G, Protti A, Blower PJ. 99mTc-bisphosphonate-iron oxide nanoparticle conjugates for dual-modality biomedical imaging. *Bioconjug Chem*. 2011;22(3): 455–465.
13. Hahn MA, Singh AK, Sharma P, Brown SC, Moudgil BM. Nanoparticles as contrast agents for in-vivo bioimaging: current status and future perspectives. *Anal Bioanal Chem*. 2011;399(1):3–27.
14. Wehrl HF, Judenhofer MS, Wiehr S, Pichler BJ. Pre-clinical PET/MR: technological advances and new perspectives in biomedical research. *Eur J Nucl Med Mol Imaging*. 2009;36(suppl 1):S56–S68.
15. Wadas TJ, Wong EH, Weisman GR, Anderson CJ. Coordinating radiometals of copper, gallium, indium, yttrium, and zirconium for PET and SPECT imaging of disease. *Chem Rev*. 2010;110(5):2858–2902.
16. Werner RA, Bluemel C, Allen-Auerbach MS, Higuchi T, Herrmann K. (68)Gallium- and (90)Yttrium-/(177)Lutetium: "theranostic twins" for diagnosis and treatment of NETs. *Ann Nucl Med*. 2015;29:1–7.
17. Stelter L, Pinkernelle JG, Michel R, et al. Modification of aminosilanized superparamagnetic nanoparticles: feasibility of multimodal detection using 3T MRI, small animal PET, and fluorescence imaging. *Mol Imaging Biol*. 2010;12(1):25–34.

18. Thorek DLJ, Ulmert D, Diop N-FM, et al. Non-invasive mapping of deep-tissue lymph nodes in live animals using a multimodal PET/MRI nanoparticle. *Nat Commun*. 2014;5:3097.
19. Kiessling F, Mertens ME, Grimm J, Lammers T. Nanoparticles for imaging: top or flop? *Radiology*. 2014;273(1):10–28.
20. Errante Y, Cirimele V, Mallio CA, Di Lazzaro V, Zobel BB, Quattrocchi CC. Progressive increase of T1 signal intensity of the dentate nucleus on unenhanced magnetic resonance images is associated with cumulative doses of intravenously administered gadodiamide in patients with normal renal function, suggesting dechelation. *Invest Radiol*. 2014;49(10):685–690.
21. Kanda T, Ishii K, Kawaguchi H, Kitajima K, Takenaka D. High signal intensity in the dentate nucleus and globus pallidus on unenhanced T1-weighted MR images: relationship with increasing cumulative dose of a gadolinium-based contrast material. *Radiology*. 2014;270(3):834–841.
22. FDA Drug Safety Communication: FDA strengthens warnings and changes prescribing instructions to decrease the risk of serious allergic reactions with anemia drug Feraheme (ferumoxytol). Published March 30, 2015. US Department of Health and Human Services; US Food and Drug Administration. Available from: http://www.fda.gov/Drugs/DrugSafety/ucm440138.htm. Accessed January 11, 2017.
23. Stendahl JC, Sinusas AJ. Nanoparticles for cardiovascular imaging and therapeutic delivery, part 1: compositions and features. *J Nucl Med*. 2015;56(10):1469–1475.
24. Bryce NS, Pham BTT, Fong NWS, et al. The composition and end-group functionality of sterically stabilized nanoparticles enhances the effectiveness of co-administered cytotoxins. *Biomater Sci*. 2013;1(12):1260–1272.
25. Pham BTT, Such CH, Hawkett BS. Synthesis of polymeric Janus nanoparticles and their application in surfactant-free emulsion polymerizations. *Polym Chem*. 2015;6(3):426–435.
26. Normandin MD, Yuan H, Wilks MQ, et al. Heat-induced radiolabeling of nanoparticles for monocyte tracking by PET. *Angew Chem Int Ed Engl*. 2015;54(44):13002–13006.
27. Boros E, Bowen AM, Josephson L, Vasdev N, Holland JP. Chelate-free metal ion binding and heat-induced radiolabeling of iron oxide nanoparticles. *Chem Sci*. 2015;6(1):225–236.
28. Ščasnár V, Lier JE. The use of SEP-PAK Sl cartridges for the preparation of gallium chloride from the citrate solution. *Eur J Nucl Med Mol Imaging*. 1993;20(3):1.